Neutron-scattering studies of binary mixtures in silica gels

B.J. Frisken
Department of Physics, Simon Fraser University, Burnaby, British Columbia, Canada V5A 1S6

David S. Cannell
Department of Physics, University of California, Santa Barbara, California 93106

M.Y. Lin and S.K. Sinha
Exxon Research and Engineering, Annandale, New Jersey 08801
(Received 26 May 1994; revised manuscript received 16 February 1995)

We report the results of neutron-scattering experiments designed to probe structure in binary mixtures confined in silica gels over the wavelength range 60–2000 Å. In what would be the one-phase region of the pure system, the scattering can be fit very well to the sum of three contributions: critical fluctuations of the mixture, preferentially adsorbed fluid, and the silica gel itself. By interpreting the adsorption as the response of the order parameter to an imposed field due to the gel, we find that the q dependence of the response is consistent with linear response theory on all length scales accessible in these experiments, although the amplitude of the response does not diverge as strongly as does the order-parameter susceptibility. In what would be the two-phase region of the pure system, we observe changes in the scattering that are consistent with the existence of large, slowly coarsening domains. The results are discussed in the context of the random-field Ising model and its magnetic realizations.

PACS number(s): 64.70.Ja, 61.43.Hv

I. INTRODUCTION

Although critical phenomena are well understood in pure systems [1] such as fluids, fluid mixtures, magnets, and superfluids, the effect of quenched disorder (such as spatially fixed impurities or fields) on critical phenomena and phase separation is only partially understood [2,3]. In antiferromagnets doped with nonmagnetic impurities, the exchange interaction is randomized and the application of an external uniform magnetic field generates a random ordering field as well. Both random-exchange and random-field models have been studied extensively and have contributed to the understanding of the behavior of doped magnets. Apparently related phenomena are observed when fluids, fluid mixtures, or superfluid helium are exposed to fixed impurities. In the case of fluids and mixtures, the impurities attract the fluid molecules or preferentially attract one species of a mixture and thus may be modeled in terms of localized fields, i.e., perturbations of the local chemical potential. This insight led Brochard and de Gennes [4] to suggest that mixtures or pure fluids confined in porous media might fruitfully be thought of within the framework of the random-field Ising model (RFIM).

In addition to the possible connection to magnetic systems and the RFIM, there are several other reasons why understanding the effects of porous media on critical phenomena and phase separation is a fundamental and interesting problem. The current understanding of critical phenomena, which is considered to be one of the great achievements of statistical physics during this century, encompasses the properties of thermal fluctuations and the response of such systems to fields that are sufficiently weak that linear response theory is appropriate. Relatively little work has been done in regard to the response to strong fields and yet strong fields are almost certainly the norm near solid substrates. In addition, strong surface fields are involved in wetting and adsorption phenomena, so that knowledge gained in studying fluids in gels might ultimately improve the understanding of wetting. Finally, gel-fluid systems exhibit a phenomenon analogous to capillary condensation, except that the condensation process is reversible and exhibits no hysteresis [5,6]. Thus a thorough exploration of the properties of gel-mixture systems may ultimately contribute to a unification of understanding with regard to wetting, critical adsorption, and capillary condensation.

It is also worth pointing out that it may be advantageous to study critical fluids in order to achieve a better understanding of the general properties of fluids and fluid mixtures confined in porous media. Surface tension, wetting forces, and bulk free energy contributions are all significant in determining morphology as well as dynamics for such systems. The critical region should prove to be a useful testing ground, possibly leading to an increased understanding of more complex systems, since it is possible to alter the relative importance of interfacial tension and wetting forces quite significantly in the vicinity of the critical point simply by changing the temperature a few degrees. The universal aspects of critical phenomena in pure systems coupled with current understanding of the critical region should also be useful in elucidating which aspects of the behavior of confined fluids will be similar for all fluids and which will not.

A considerable number of experiments have been carried out to date attempting to understand the behavior of pure fluids, mixtures, and superfluid helium, either confined in porous glasses or containing the interconnected strands of a gel [7–9,5,10–12]. Several features, including enhanced scattering due to a static response to the field imposed by the medium and the history-dependent behavior within the two-phase boundary of the pure system, are consistent with features predicted for the RFIM [13,14] and observed in random-field magnets [15–18]. However, no obvious mapping of all fluids in porous media systems onto the RFIM has been demonstrated to date [19]. In certain porous media, particularly those of low porosity, the effects of confinement in the pores may be more important than the effects of randomness. For example, if the correlation length of the fluid does not grow beyond the pore size, the fluctuations will not sample the randomness. This appears to be the case for binary fluid mixtures confined in Vycor glass [8,9]. The effects of confinement can apparently resemble some of those associated with the RFIM, namely, microphase (rather than macrophase) separation, hysteretic behavior, and slow relaxation effects [20]. However, the physical origins are rather different. For more open porous structures, the effects of both randomness and excluded volume may be important since the correlation length associated with the concentration fluctuations can span large inhomogeneous regions.

It is also clear that the RFIM fails to incorporate a number of features that might possibly be relevant for the fluid systems. For example, in fluid systems the field does not have a symmetric probability distribution; a randomly chosen location in a sample containing a dilute porous material has a high probability of corresponding to a very small field and a very small probability of corresponding to a high field [21]. In addition, spatial randomness does not persist on all length scales for any porous material or gel network. Silica gels, for example, exhibit density fluctuations that are power-law correlated over distances up to a cutoff, or gel correlation length ξ_G, which may be anywhere from 100 Å to a few micrometers [22]. In treatments of the RFIM the length scale of the random field is assumed to be smaller than the critical system's correlation length ξ; however, binary fluid systems in silica gel appear to phase separate (at least microscopically) before ξ exceeds ξ_G [10,11]. In addition, a network or porous medium excludes the critical system from the region it occupies. The effect of such exclusion on the buildup of critical correlations is not obvious. Furthermore, two characteristics of fluids might alter the dynamics predicted by the RFIM. Fluid systems have conserved order parameters so that fluctuations can decay only by diffusion rather than simple spin flip processes. Consequently, long-wavelength variations in concentration might be expected to decay extremely slowly. Dynamics might also be affected by boundary conditions that require zero flow velocity at the surface of any rigid porous medium. Presumably, the effect would be much more severe for diffusion within the restricted pore space of Vycor glass than within a very open material such as a dilute gel.

Silica networks are a practical example of an open porous structure that offer a convenient method of exposing critical fluids and mixtures to fields that are locally strong while at the same time spatially dilute. Furthermore, the spatial distribution of silica on length scales relevant to critical phenomena has been extensively characterized by light and neutron scattering. Previous studies of the effect of dilute silica gel on the critical phenomena of binary fluid mixtures include light-scattering measurements on mixtures of lutidine and water [10] and isobutyric acid and water [11] imbibed in silica gels. The lutidine-water studies, made primarily in what would be the one-phase region of the pure system, showed that the intensity scattered from the gel-mixture samples had very nearly the same q dependence as that from silica gels containing only water, while the magnitude of the scattering increased strongly as the two-phase region of the pure system was approached. This behavior was interpreted as the result of preferential attraction of lutidine by the silica. In the critical region this results in the buildup of a lutidine-rich region near the silica and this region should extend further and further from the silica as the critical point is approached. In fact, it is well known that surfaces inevitably attract one of two species preferentially or prefer either liquid or vapor phase when in contact with a single fluid [23]. For example, in a critical system near a *planar* substrate, the composition of the mixture varies smoothly over a distance from the substrate comparable to the bulk correlation length and the amount of adsorbed material diverges as the critical point is approached [24]. This phenomenon is known as critical adsorption. If the surfaces of the gel are modeled in terms of a surface field that acts on molecules or atoms near the surface, then the resulting perturbation of the concentration is the static response of the order parameter of the mixture, i.e., its concentration, and this response becomes increasingly strong in the vicinity of the pure system's critical point. The fluctuations in silica concentration are correlated only over a distance ξ_G and are spatially random for length scales in excess of ξ_G. Thus one may view the gel as imposing fields that are spatially random on scales above ξ_G. In q space, these fields have a q-independent rms amplitude for $q \leq \xi_G^{-1}$ and fall off rapidly in amplitude for $q > \xi_G^{-1}$.

In addition to a static component, the scattered light generally contained a time-dependent part. In lutidine-water-gel samples, no time-dependent scattering was observed, but studies of isobutyric acid and water in silica gel [11] allowed measurement of the time-dependent component and its identification with critical concentration fluctuations. However, no true critical slowing down has been found in gel-mixture systems. The diffusion coefficient, which goes to zero at the pure system's critical point, decreases strongly in its vicinity for the isobutyric acid-water-gel system, but the system undergoes a phase separation process before the diffusion coefficient reaches zero. Since the diffusion coefficient varies as the inverse of the correlation length, at least for the pure system, this behavior is consistent with no true divergence of the correlation length. The phase separation occurs when the correlation length of the mixture (as obtained from

the diffusion coefficient) has grown to the point where it is comparable to ξ_G.

These observations can be compared to studies of diluted antiferromagnets in the presence of an external field, an experimental manifestation of the RFIM. The static response of the fluid system is reminiscent of the static response of a magnet to a random field, with the additional complexity that the field imposed by the silica is spatially correlated. Although the identification of both static and time-dependent components has not been achieved for magnetic systems, the presence of both Lorentzian-squared and Lorentzian components in neutron scattering from magnetic systems in the paramagnetic phase is consistent with scattering that originates from both a static response to the random field and residual critical fluctuations [15]. In the gel-mixture systems, phase separation occurs before the correlation length of the mixture can diverge, reminiscent of the magnetic systems that enter a frozen-domain state above the expected critical point of the random-field system. In the fluid case, however, the domains clearly evolve with time, albeit slowly, as the samples do eventually clear. Consequently, it should be possible to study their relaxation from the frozen-domain state to the equilibrium state.

In the gel-mixture studies, the static response of the fluid system to the gel was interpreted in terms of a simple model in which fluctuations in the local silica concentration induce time-independent fluctuations in the concentration of the preferentially attracted species [10]. This model results in an expression for the scattering from the gel-mixture system in terms of the scattering from the gel-water system and a temperature dependent response function $\alpha(T)$. However, very close to the critical region, it was evident from the light-scattering data that the static response function $\alpha(T)$ was developing a q dependence [11]. Although the scattered intensity continued to increase as the critical region was approached, there were larger increases in the intensity at low q than at high q and thus the q dependence of the time-independent scattering began to deviate from that of the gel-water samples. This behavior was not unexpected since the linear response of a critical system to an applied field becomes strongly q dependent in the critical region, with response falling off for q values in excess of ξ^{-1}.

In order to study the spatial dependence of the concentration fluctuations on smaller length scales, it was thus decided to carry out small-angle neutron-scattering (SANS) experiments on the lutidine-water-gel system. Previous SANS experiments on binary fluid phase separation in porous media focused on the lutidine-water-Vycor glass system [8,9]. These experiments showed an adsorbed lutidine-rich layer on the pore surfaces and a correlation length smaller than the pore-size in the single-phase region and, in the two-phase region of the pure system, microdomains restricted to the pore size and lutidine-rich wetting layers on the Vycor glass. Vycor glass, with a porosity of only $\sim 28\%$, represents the opposite (high confinement) limit to that encountered in the present system, which has porosities ranging from 98% to 99.5%.

The present studies of the lutidine-water-gel system show that, for temperatures sufficiently far from the critical region, the q dependence of the scattering is almost identical to that of the gel-water system over the entire q range studied. As the critical region is approached, the absolute scattering increases more strongly at low q than at high q. The q range over which the scattering shows a tendency to saturate moves down to lower and lower q as the critical region is approached. Although the present experiments cannot resolve the scattering into a static and a time-dependent component, the data in the one-phase region are fit very well by a form that allows for both scattering from critical fluctuations and a contribution resulting from a response of the system to the fields due to the gel. We find that the effective values for the correlation length of the critical fluctuations of the confined mixture and the length scale describing the q dependence of the static response function $\alpha(q,T)$ can be set equal in the one-phase region without significantly degrading the fit quality. In addition, the susceptibility χ and correlation length ξ are roughly comparable to those of the pure system and, as expected, χ increases as ξ^2 near the two-phase boundary of the pure system to within experimental error. However, the amplitude of the static response $\alpha(0,T)$ does not increase as strongly as does the susceptibility in the vicinity of the critical point and in fact the ratio $\alpha(0,T)/\chi$ appears to approach zero near what would be the critical point of the pure mixture.

Since the integrated scattering cross section of this system is much less for neutrons than it is for light, we have been able to study the scattering in what would be the two-phase region of the pure system, which for light is generally obscured by multiple scattering. Here we observe a change in the structure factor from that in the one-phase region consistent with the existence of large domains, which coarsen slowly over time.

As well as studying the gel-mixture system in both the one- and the two-phase regions of the phase diagram, we have measured the structure factor of several gels. This extends to higher q a previous light-scattering investigation [22] where these gels were observed to scatter like mass fractals on length scales shorter than ξ_G and isotropically for $q \leq \xi_G^{-1}$. The neutron-scattering studies confirm this picture and show that the fractal behavior extends to the smallest length scales accessible here, corresponding to fluctuations with wavelengths of 60 Å.

II. EXPERIMENT

A. Sample preparation

The silica gels were made by polymerization of a silica precursor (tetramethylorthosilicate) in deuterated water (D_2O) by a two-step process [25]. The gelling solution was introduced directly into cells designed for neutron scattering. Each cell consisted of an anodized aluminum block designed to hold two circular windows 1.0 mm apart. The cells were assembled with viton O rings and

quartz windows that were 1.6 mm thick. This resulted in sample volumes 2.5 cm in diameter and 0.10 cm thick. The gels were never dried. Some samples were set aside to be used strictly for studies of the gel structure, while a binary fluid mixture was introduced into other gel samples for gel-mixture studies. Gels containing 4.0 wt. % (2.05 vol %) silica were primarily used in the later studies. These gels typically have a fractal correlation length of ~ 250 Å, which is comparable to the correlation length of binary mixtures about 1° from the coexistence curve. To introduce the mixture into the gel, one of the quartz windows was removed, without disturbing the gel, and mixture was placed over the gel. The mixture was subsequently stirred occasionally and changed three times over the course of four days. The shallow depth of the sample led to rapid equilibration of the concentration of the mixture in the gel with the supernatant. After equilibration, the supernatant was poured off and the sample was resealed. The binary mixture used was 2,6-lutidine and D_2O at weight fractions w ranging from 0.18 to 0.37 lutidine. [Concentration will mainly be reported here in volume fractions ϕ, where the volume fraction of A in a mixture of A and B is given by $\phi = w_A/(w_A+w_B\rho_A/\rho_B)$, with ρ_A (w_A) and ρ_B (w_B) being the densities (weight fractions) of A and B, respectively.] Lutidine and D_2O, like lutidine and H_2O, have an inverted coexistence curve, so that the two-phase region is approached from lower temperatures. The critical temperature and lutidine concentration, as observed in cloud-point measurements of pure mixtures, are 28.2 °C and 30 vol %, respectively.

B. Apparatus

Measurements were made at the Cold Neutron Research Facility at the National Institute of Standards and Technology (NIST) on the 30-m NIST–Exxon–University of Minnesota SANS instrument. A range of q from 0.003 to 0.1 $Å^{-1}$ was obtained using neutrons of wavelength λ=7.0 Å ($\Delta\lambda/\lambda = 0.14$) and two source-sample-detector setups. In the first setup (high resolution), the source aperture diameter was 2.20 cm, the source aperture to sample aperture distance was 1631 cm, the sample aperture to detector distance was 1536 cm, and the sample aperture diameter was 1.27 cm. For the second setup (low resolution), the appropriate specifications were 5.00 cm, 701 cm, 371 cm, and 1.27 cm, respectively. The samples were mounted in a multichambered temperature-controlled housing, which kept the temperature stable to better than ±0.1 °C.

C. Sample measurement

The samples were oriented with the incident neutron beam normal to the quartz windows. Neutrons scattered by the sample were detected by a position sensitive ^3He area detector. Low resolution measurements typically required about 10 min per sample to accumulate suitable statistics, while high resolution measurements took about 30 min. The scattering from NIST standard samples was used to calibrate the instrument. The data were corrected for detector response, background, and empty cell scattering and converted to an absolute intensity scale by comparing to the standard samples.

The silica gel samples were measured at room temperature. The gel-mixture samples were measured at various temperatures in the one- and the two-phase regions of the pure system. After the measurements were finished, these samples were analyzed by gas chromatography to determine the lutidine concentration in the gels [10]. Measurements were also made of pure mixtures with concentrations spanning the critical region so that the critical behavior of the mixture with and without the gel could be compared.

III. RESULTS AND DISCUSSION

A. Silica gels

Figure 1 shows data for the scattering cross section per unit volume of sample $S(q)$ for silica gels made in D_2O containing 0.506%, 1.02%, and 2.05% silica by volume, but made at similar pH. Figure 2 shows similar data for gels containing 2.05 vol % silica but made over a range of pH values. We find that $S(q)$ is well described by the function [26]

$$S(q) = B + \frac{S(0)}{\left[1+q^2\xi_G{}^2\right]^{(D_f-1)/2}} \times \frac{\sin\left[(D_f-1)\tan^{-1}(q\xi_G)\right]}{(D_f-1)q\xi_G}, \quad (1)$$

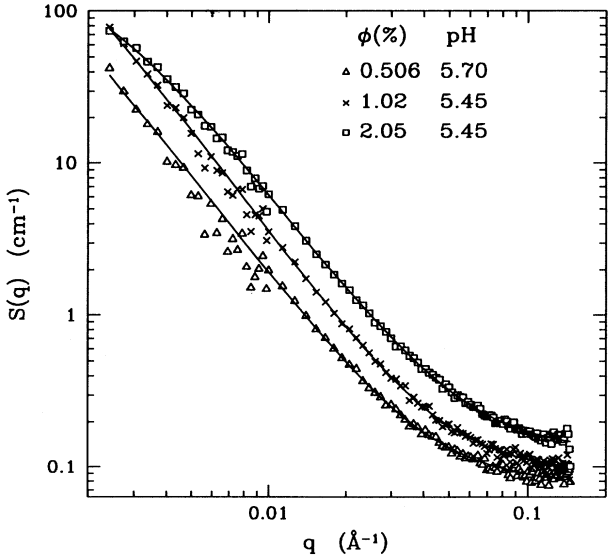

FIG. 1. Absolute neutron-scattering cross section per unit volume measured for three silica gel samples in D_2O made with different concentrations of silica. The silica volume fraction and pH of the gelling solution are shown on the graph. The solid curves are fits of Eq. (1) to the data.

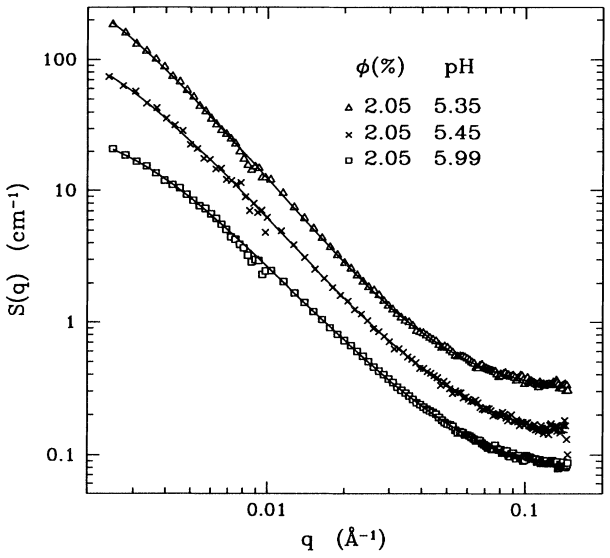

FIG. 2. Absolute neutron-scattering cross section per unit volume measured for three silica gel samples made in D_2O at different pH. The silica volume fraction and pH of the gelling solution are shown on the graph. The data for the pH 5.35 sample have been multiplied by a factor of 2.0 and the data for the pH 5.99 sample have been divided by a factor of 2.0, to prevent overlap of the data sets at high q. The solid curves are fits of Eq. (1) to the data.

where ξ_G, the gel correlation length, represents the large length scale limit of the fractal correlations, D_f is the fractal dimension, $S(0)$ represents the $q \to 0$ limit of the coherent scattering, and B is a background term that accommodates the incoherent scattering contribution. The solid lines in the two figures are the results of fitting Eq. (1) to the data, which clearly provides an excellent fit [27]. This form, without the background term, had been shown previously to accurately characterize the light-scattering from this type of silica gel over a wide range of silica concentrations and gelation conditions [22]. It is the Fourier transform of the density-density correlation function

$$g(r) \equiv \langle \delta\phi(r)\delta\phi(0)\rangle = A\,\frac{\bar{\phi}^2 e^{-r/\xi_G}}{(r/\xi_G)^{3-D_f}}, \qquad (2)$$

where $\delta\phi(r)$ is the local deviation from the sample average concentration of silica $\bar{\phi}$ and A is a constant, which the previous light-scattering measurements showed to be equal to 1.8. The angular brackets represent an ensemble average. The fact that the data for $S(q)$ are well fit by Eq. (1) shows that fluctuations in local silica concentration are correlated up to distances of order ξ_G, with correlation falling off rapidly for length scales larger than ξ_G. This form of correlation function is characteristic of a mass fractal, with the fractal behavior existing for length scales shorter than ξ_G. Generally, the fractal behavior persists to larger length scales in gels made at smaller silica concentration. Since the two lowest concentration gels measured here have correlation lengths that are too large to be accessible by neutron scattering, ξ_G was fixed in these cases at values consistent with results from the previous light-scattering studies of such gels [22]. The particular choice of ξ_G affects $S(0)$, but does not have a significant effect on D_f. Table I summarizes the fit parameters for the gels measured in these experiments.

In the light-scattering studies of this type of silica gel [22], it was found that ξ_G could be varied from 100 Å to 2 μm by decreasing the concentration of silica in the gelling solution. For a given concentration, ξ_G could also be varied by changing the pH of the gelling solution. It was also observed that the result obtained for D_f by fitting the light scattering data to Eq. (1) (without the background term) was correlated with ξ_G, increasing from 2.1 in the most dilute solution measured (0.091 vol%) to 2.3 in the samples with the smallest ξ_G for which D_f could be determined with any confidence. (As ξ_G decreases, the range of q values over which the data exhibit behavior of the q^{-D_f} form becomes too small to enable one to determine D_f.)

The results summarized in Table I show that the variation of ξ_G with concentration and pH is consistent with that observed in Ref. [22]. On the other hand, there does not seem to be any significant variation of D_f with ξ_G, as all of the measured values fall in the range of 2.1±0.1. There is no evidence of a trend to higher D_f with lower ξ_G as was observed in the previous light-scattering study. Since the current experiments allow access to the q range over which the fractal nature of the more concentrated gels is manifest, these measurements of the fractal dimension should be more accurate for such gels. We conclude that the fractal dimension, at least for gels made in D_2O, is constant at these concentrations and has a value of 2.1±0.1. The difference between the results obtained by fitting only low-q (light-scattering) data and

TABLE I. Parameters resulting from fitting Eq. (1) to the data for silica gels. An asterisk indicates value held constant in fit.

vol% silica	pH	$S(0)$ (cm^{-1})	ξ_G (Å)	D_f	B (cm^{-1})
0.506	5.70	1259 ± 66	2000*	2.13 ± 0.01	0.076 ± 0.001
1.02	5.45	717 ± 21	1000*	2.21 ± 0.01	0.091 ± 0.001
1.02	5.56	595 ± 22	1000*	2.19 ± 0.01	0.120 ± 0.001
2.05	5.35	327 ± 30	546 ± 25	2.22 ± 0.01	0.146 ± 0.001
2.05	5.45	190 ± 14	473 ± 22	2.13 ± 0.01	0.128 ± 0.002
2.05	5.99	75.5 ± 3.4	358 ± 12	2.03 ± 0.01	0.140 ± 0.001

the present data extending to much higher q may indicate that Eq. (1) does not provide a perfect description of the crossover region near $q = \xi_G^{-1}$ or possibly that gels grown in D_2O differ slightly from those grown in H_2O. This is of no relevance for the current investigation however.

The short length scale studies of the silica gels reported here show that the model of a fractal structure for the silica gel expressed in Eq. (1) continues to accurately represent the data down to the smallest length scales available in these measurements. There is no evidence of a change in the structure at small length scales, which one could attribute to a well defined cross-sectional dimension for the silica strands. Nor is there any indication of a crossover to q^{-4} behavior, which would correspond to scattering from sharp interfaces [28]. These studies show that such structure, if it exists at all, occurs for length scales smaller than about 10 Å ($1/q_{\max}$).

B. Gels with binary fluid mixture

1. One-phase region

The scattering from gel samples containing fluid mixtures was observed to change with temperature, as expected. Figure 3 shows results for a sample containing 2.05 vol% silica and 40 vol% lutidine at various temperatures approaching, from the one-phase region, the coexistence curve of the pure mixture. The silica gel was from the same batch as the 2.05 vol% silica gel made at pH=5.45 shown in Figs. 1 and 2; the lower data set in Fig. 3 reproduces the data for the gel-D_2O sample itself. At temperatures well below the critical temperature, the gel-mixture sample scatters more than the gel-D_2O sample, but the q dependence of the scattering is nearly identical to that of the gel-D_2O sample. As the temperature is increased towards the coexistence curve, the intensity increases, but it increases more rapidly at low q than at high q. As part of the same run, measurements were made on 2.05 vol% silica samples containing 37 and 43 vol% lutidine. These samples were in gels from the same batch as the one containing 40 vol% lutidine. All of these samples showed the same basic behavior, throughout the one-phase region.

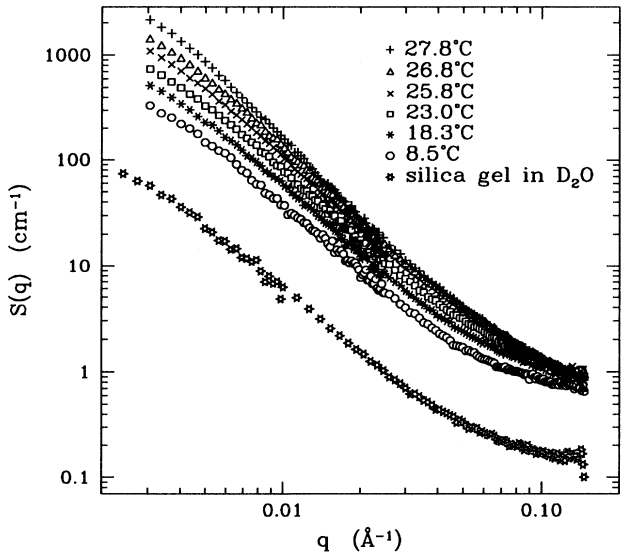

FIG. 3. Absolute neutron-scattering cross section per unit volume measured for a gel-mixture sample containing 2.05 vol% silica and 40 vol% lutidine at various temperatures. Far from the critical region of the pure mixture, the q dependence of the scattering is similar to that of the gel-D_2O sample. As the critical region is approached, the scattering increases at low q, but tends to saturate at high q. The lowest curve shows the scattering from a silica gel from the same batch but containing only D_2O.

The scattering results for all of these samples can be interpreted quantitatively using a generalization of the model used previously to interpret the intensity of light scattered from similar samples [10]. In general, neutrons are scattered from fluctuations in the local scattering length density. The scattering cross section per unit volume $S(q)$ is equal to the spatial Fourier transform of the scattering length autocorrelation function

$$S(\vec{q}) = \int \langle \delta\rho(0)\ \delta\rho(\vec{r})\rangle\ e^{-i\vec{q}\cdot\vec{r}}\ d\vec{r} = \frac{1}{V}\langle \delta\rho(\vec{q})\ \delta\rho^*(\vec{q})\rangle, \tag{3}$$

where $\delta\rho(\vec{r})$ is the local fluctuation in the scattering length density about the global average and V is the volume of the sample illuminated by the neutron beam. For these samples, the fluctuations in scattering length density are almost entirely the result of concentration fluctuations.

The scattering length density can be written as the volume-fraction weighted average of the individual scattering length densities of silica, lutidine, and D_2O: $\rho_s = 3.64 \times 10^{10}$ cm^{-2}, $\rho_l = 1.15 \times 10^{10}$ cm^{-2}, and $\rho_{hw} = 6.38 \times 10^{10}$ cm^{-2}, respectively,

$$\rho(\vec{q}) = \rho_s\phi_s(\vec{q}) + \rho_l\phi_l(\vec{q}) + \rho_{hw}\phi_{hw}(\vec{q}), \tag{4}$$

where $\phi(\vec{q})$ is the $\vec{q}$th spatial Fourier component of the volume fraction of each component. In terms of concentration fluctuations, this may be rewritten as

$$\delta\rho(\vec{q}) = (\rho_s - \rho_{hw})\delta\phi_s(\vec{q}) + (\rho_l - \rho_{hw})\delta\phi_l(\vec{q}), \tag{5}$$

since $\delta\phi_s + \delta\phi_l + \delta\phi_{hw} = 0$.

Following the previous light-scattering work, we decompose the fluctuations in lutidine concentration, $\delta\phi_l(\vec{q})$ into a static (time-independent) response of the mixture to the gel, which we denote $\delta\phi_l^{\rm stat}(\vec{q})$, and a fluctuating (time-dependent) term, which we denote $\delta\phi_l^{\rm fluct}(\vec{q})$, imagining it to represent the remaining critical fluctuations,

$$\delta\phi_l(\vec{q}) = \delta\phi_l^{\rm fluct}(\vec{q}) + \delta\phi_l^{\rm stat}(\vec{q}). \tag{6}$$

From measurements of the concentration of the mixture in the gel by gas chromatography, we know that lutidine was preferentially adsorbed in these experiments.

We can then relate the time-independent concentration fluctuations to the quenched disorder, i.e., to the static fluctuations in local silica volume fraction, by

$$\delta\phi_l^{\text{stat}}(\vec{q}) \equiv \alpha(\vec{q},T)\,\delta\phi_s(\vec{q}), \tag{7}$$

which defines the temperature and wave-vector-dependent response function $\alpha(\vec{q},T)$, characterizing the response of the order parameter (ϕ_l) to the perturbing field imposed by the gel. Note that Eq. (7) corresponds to a convolution in real space and thus to a possibly non-local response function. The q dependence of the local scattering length density fluctuations can then be written

$$\delta\rho(\vec{q}) = (\rho_l-\rho_{hw})\delta\phi_l^{\text{fluct}}(\vec{q}) + [(\rho_s-\rho_{hw}) + (\rho_l-\rho_{hw})\;\alpha(\vec{q},T)]\,\delta\phi_s(\vec{q}). \tag{8}$$

Using Eqs. (3) and (8), the scattering cross section per unit volume can be expressed as

$$S(q) = \frac{1}{V}[(\rho_l-\rho_{hw})^2\,\langle\delta\phi_l^{\text{fluct}}(q)\;\delta\phi_l^{*\text{fluct}}(q)\rangle + [(\rho_s-\rho_{hw}) + (\rho_l-\rho_{hw})\;\alpha(q,T)]^2 \times\langle\delta\phi_s(q)\;\delta\phi_s^*(q)\rangle], \tag{9}$$

provided we assume that the static and time-dependent concentration fluctuations are uncorrelated.

To simplify the first term in Eq. (9), we assume that the scattering from the time-dependent critical fluctuations has the Ornstein-Zernike form

$$\frac{1}{V}\;\langle\delta\phi_l^{\text{fluct}}(q)\;\delta\phi_l^{*\text{fluct}}(q)\rangle \;=\; \frac{\chi(T)}{1+q^2\;\xi(T)^2}, \tag{10}$$

where χ is the susceptibility and ξ is the correlation length of the mixture. The susceptibility is related to the osmotic susceptibility

$$\tilde{\chi} = \frac{k_BT}{n}\;\left(\frac{\partial X}{\partial\mu}\right)_{P,T} \tag{11}$$

through

$$\chi \;=\; \frac{\phi_l(1-\phi_l)}{X_l(1-X_l)}\,\tilde{\chi}, \tag{12}$$

where X_l is the mole fraction of lutidine, n is the number density of the mixture, and μ is the difference of the chemical potentials of the two components of the mixture [29]. In a pure fluid, both χ and ξ diverge as the critical point is approached.

We can simplify the second term of Eq. (9) by noting that the measured scattered cross section per unit volume for the gel containing only D_2O is just

$$S(q)_{ghw} \;=\; \frac{1}{V}\;(\rho_s-\rho_{hw})^2\;\langle\delta\phi_s(q)\;\delta\phi_s^*(q)\rangle, \tag{13}$$

so that the second term of Eq. (9) can be written in terms of $S(q)_{ghw}$ and the response function $\alpha(q,T)$. Adding a background term B to allow for incoherent scattering leads to a fitting function of the form

$$S(q) \;=\; B \;+\; \frac{(\rho_l-\rho_{hw})^2\;\chi}{1+q^2\;\xi^2} + \left[1+\frac{\rho_l-\rho_{hw}}{\rho_s-\rho_{hw}}\alpha(q,T)\right]^2\;S(q)_{ghw}. \tag{14}$$

$S(q)_{ghw}$ was found by fitting Eq. (1) to data for the appropriate gel-D_2O sample and subtracting the background. To fit Eq. (14) to the gel-mixture data, we need only assume a q dependence for the static response function $\alpha(q,T)$. A linear response of the order parameter to the field imposed by the gel would result in a response function containing a term of the Ornstein-Zernike form

$$\alpha(q,T) = -\frac{\bar{\phi}_l}{\bar{\phi}_l+\bar{\phi}_{hw}} + \frac{\alpha_0(T)}{(1+q^2\;\xi^2)}, \tag{15}$$

where a bar denotes a sample average. The first term is just the negative of the average volume fraction of lutidine in the fluid mixture $\bar{\phi}_l^{\text{mixt}}$. It accounts for the fact that since silica excludes the mixture from the space it occupies, the local volume fraction of lutidine, as well as that of water, must decrease as that of silica increases, in the absence of any adsorption [30]. It is included explicitly in order to force the case of no adsorption to correspond to $\alpha_0(T) = 0$. The second term is the linear Ornstein-Zernike response; if the response is actually linear, $\alpha_0(T)$ should be proportional to χ and $\alpha(q,T)$ should exhibit the same length scale as do the critical fluctuations. We are thus led to a fitting function of the form

$$S(q) \;=\; B \;+\; \frac{(\rho_l-\rho_{hw})^2\;\chi}{(1+q^2\;\xi^2)} \;+\; \left[\frac{\rho_s-\bar{\rho}^{\text{mixt}}}{\rho_s-\rho_{hw}} + \frac{\rho_l-\rho_{hw}}{\rho_s-\rho_{hw}}\,\frac{\alpha_0(T)}{(1+q^2\;\xi^2)}\right]^2\;S(q)_{ghw}, \tag{16}$$

where $\bar{\rho}^{\text{mixt}}$ is the scattering length density of the fluid mixture, averaged over the volume occupied by fluid only,

$$\bar{\rho}^{\text{mixt}} = \frac{\rho_l\;\bar{\phi}_l+\rho_{hw}\;\bar{\phi}_{hw}}{\bar{\phi}_l+\bar{\phi}_{hw}}. \tag{17}$$

Equation (16) is similar in functional form to expressions used to fit neutron-scattering data for diluted uniaxial antiferromagnets in an external magnetic field [15]. In the one-phase region, these forms correspond to the sum of a Lorentzian $(q^2+\kappa^2)^{-1}$ and a Lorentzian-squared term $(q^2+\kappa^2)^{-2}$, where κ^{-1} is the correlation length. The Lorentzian represents the scattering from critical fluctuations and the Lorentzian-squared term arises from the static response of the system to the random field. In the magnetic case, the random field is spatially uncorrelated and hence is q independent. The present form is more complicated because of the correlated nature of the field due to the gel and because scattering from the gel itself must be taken into account. In addition, the form of Eq. (16) is similar to responses predicted for fluids in porous networks based on extensions of the RFIM [13,14].

Equation (16) has four adjustable parameters B, χ, ξ, and α_0 and it provided a nearly perfect fit to data taken for a number of samples spanning a wide temperature and concentration range throughout the one-phase region of the pure system. The quality of the fits was very high, as shown by the typical fit and residuals illustrated in Fig. 4. The lower portion of the figure shows the deviation of the data from the fit in units of the standard deviation σ of the data, which was set equal to the square root of the number of counts collected for each data point.

Fitting Eq. (16) to the data allows the effective susceptibility χ and correlation length ξ characterizing the critical fluctuations of the binary fluid in the presence of the silica gel to be obtained. Results for the three samples containing 37, 40, and 43 vol% lutidine are given in Tables II, III, and IV, respectively. Before comparing them to results for the unconfined system, we note that preferential adsorption of lutidine causes the concentration of the nonadsorbed region, the part of the sample that is participating in critical fluctuations, to be pulled towards the D_2O-rich side of the coexistence curve as the two-phase region is approached. The severity of this effect may be estimated using the data for $\alpha_0(T)$. As shown previously [10] for a crude model in which the sample is imagined to consist of two interpenetrating regions—a region of silica and adsorbed lutidine-rich fluid, which is responsible for the static scattering, and a region of free fluid—the volume fraction of lutidine in the free fluid $\bar{\phi}_l^{\text{free}}$ is simply related to $\alpha(q=0,T)$ by

$$\bar{\phi}_l^{\text{free}} = \bar{\phi}_l - \alpha(q=0,T)\bar{\phi}_s. \tag{18}$$

Using Eq. (15), this result can be expressed as

$$\bar{\phi}_l^{\text{free}} = \bar{\phi}_l^{\text{mixt}} - \alpha_0(T)\ \bar{\phi}_s, \tag{19}$$

which allows the free fluid concentration for each sample as a function of temperature to be estimated from the data for $\alpha_0(T)$. This result is independent of the volume occupied by the adsorbed fluid or its concentration. Figure 5 shows how the concentration of lutidine in the nonadsorbed or free fluid as estimated in this manner changes with temperature for each sample. An effect of this sort must be present because the concentration of each species is globally conserved and as lutidine is adsorbed and ceases to participate in critical fluctuations [31] the remaining fluid must become depleted in lutidine. Although the model being discussed is admittedly crude, it is important to recognize the existence of such an effect because the properties of critical mixtures are dependent on both temperature and concentration in the critical region. Previous measurements [11] show that the behavior of the free fluid is consistent with this interpretation.

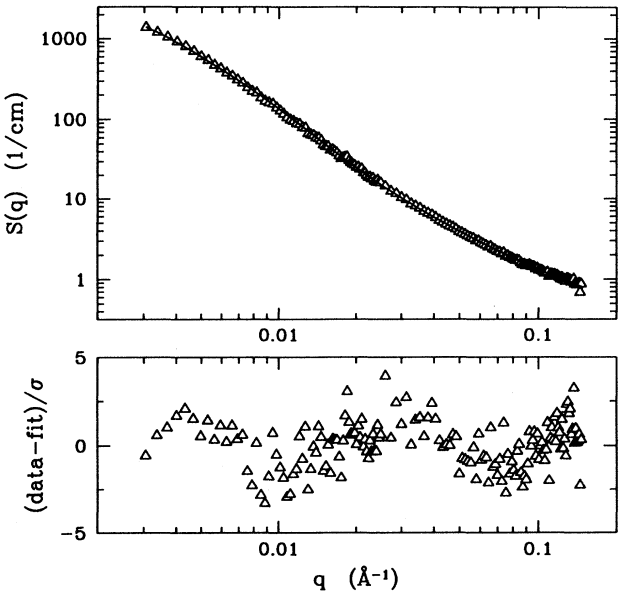

FIG. 4. Result of fitting Eq. (16) to the absolute neutron-scattering cross section per unit volume measured for a gel-mixture sample containing 2.05 vol% silica and 40 vol% lutidine at 26.80 °C. The residuals in units of the standard deviation of the data are shown in the bottom portion of the figure.

Data for pure mixtures were taken over the temperature range of 12–33 °C, covering the concentration range of 25–46 vol% lutidine. As expected, the ratio of χ/ξ^2 is basically constant for the pure mixtures independent of temperature, although some concentration dependence is apparent, as shown in Fig. 6(a). The same does not appear to be true for the gel-mixture sustem, as shown in Fig. 6(b). These results are plotted as a function of $T_c - T$, using $T_c = 28.2$ °C, the value we measured for the pure system. It is interesting to note that this ratio

TABLE II. Parameters resulting from fitting Eq. (16) to the data for the gel-mixture sample with $\bar{\phi}_l = 0.37$.

T (°C)	$\bar{\phi}_l^{\text{free}}$	χ (10^{-20} cm^3)	ξ (Å)	α_0	B (cm^{-1})
8.50	0.36	0.00938 ± 0.00401	11.4 ± 0.90	1.14 ± 0.005	0.504 ± 0.027
18.34	0.35	0.0777 ± 0.0058	21.0 ± 0.66	1.55 ± 0.005	0.425 ± 0.011
23.03	0.34	0.161 ± 0.0073	26.2 ± 0.54	1.89 ± 0.005	0.337 ± 0.009
25.84	0.33	0.333 ± 0.012	35.5 ± 0.56	2.44 ± 0.007	0.307 ± 0.009
26.80	0.32	0.518 ± 0.016	43.3 ± 0.60	2.83 ± 0.009	0.269 ± 0.009
27.76	0.31	1.01 ± 0.033	60.1 ± 0.89	3.59 ± 0.018	0.245 ± 0.010
28.75		2.93 ± 0.062	103.1 ± 0.84	5.64 ± 0.027	0.260 ± 0.015
29.71		4.78 ± 0.089	139.5 ± 0.84	9.17 ± 0.05	0.289 ± 0.016

TABLE III. Parameters resulting from fitting Eq. (16) to the data for the gel-mixture sample with $\bar{\phi}_l = 0.40$.

T (°C)	$\bar{\phi}_l^{\text{free}}$	χ (10^{-20} cm^3)	ξ (Å)	α_0	B (cm^{-1})
8.50	0.39	0.0288 ± 0.0036	15.0 ± 0.80	1.18 ± 0.004	0.568 ± 0.012
18.34	0.38	0.0964 ± 0.0066	20.9 ± 0.74	1.50 ± 0.004	0.585 ± 0.009
23.03	0.37	0.254 ± 0.015	29.4 ± 0.96	1.83 ± 0.006	0.491 ± 0.008
25.84	0.36	0.511 ± 0.027	37.8 ± 1.08	2.22 ± 0.008	0.393 ± 0.010
26.80	0.36	0.620 ± 0.027	40.5 ± 0.90	2.53 ± 0.009	0.336 ± 0.010
27.76	0.35	1.30 ± 0.068	58.3 ± 1.54	3.15 ± 0.021	0.282 ± 0.013
28.75		15.0 ± 0.53	208 ± 3.47	8.81 ± 0.15	0.402 ± 0.015
29.71		12.5 ± 0.43	204 ± 3.12	12.7 ± 0.21	0.551 ± 0.019

for the gel-mixture system approaches that of the pure system *near* the critical point and falls increasingly below it *away* from the critical point. Although this trend is well outside the limits corresponding to the statistical errors in the fitting parameters χ and ξ, we cannot rule out the possibility that it is a systematic effect resulting, for example, from an imperfect fitting function.

We may compare the results obtained for χ and ξ to those found for the pure system in two different ways. The most straightforward comparison is to consider the ratio of a quantity to that of the pure system at the same temperature and at the *average* concentration of the fluid portion of the gel-mixture sample $\bar{\phi}_l^{\text{mixt}}$. The susceptibility ratio found in this manner is displayed in Fig. 7(a). Figure 7(b) shows the same ratio, but with the pure system susceptibility at the concentration $\bar{\phi}_l^{\text{free}}$ estimated for the free fluid, i.e., at the concentration shown by the symbols in Fig. 5. Clearly the gel-mixture system behaves more like the pure system at the temperature-dependent concentration $\bar{\phi}_l^{\text{free}}$ than at the fixed concentration $\bar{\phi}_l^{\text{mixt}}$. The same comparison is shown for the correlation length in Fig. 8 and is consistent with the above interpretation.

Within the context of strictly linear response, the $q = 0$ limit of the response function $\alpha_0(T)$ should be directly proportional to the susceptibility χ. Figure 9(a) displays the ratio α_0/χ, for each of the gel-mixture samples. There is no region of temperature where α_0 is simply proportional to χ, and although α_0 increases as the critical region is approached, it does not do so nearly as strongly as does χ. In fact, as shown in Fig. 9(b), the ratio $\alpha_0(T)/\xi$ is much more nearly constant for these samples.

2. *Two-phase region*

Macroscopic phase separation occurs much more slowly in mixtures containing silica gel than it does in pure mixtures. This is easily judged by physical appearance. A sample of a pure mixture will phase separate and form macroscopic domains visible to the unaided eye in a matter of minutes for temperatures more than about 0.1 °C into the two-phase region. In contrast, samples containing even rather dilute gels remain milky in appearance for days or more, which is almost certainly the result of extremely slow domain growth following the initial decomposition or nucleation process. In light-scattering studies of similar gel-mixture systems [10,11], the onset of phase separation was identified by various changes in the behavior of the scattered light. Temperature quenches in some of the samples revealed overshoots in the scattered intensity that decayed slowly in time and were mainly visible at much smaller-q values than are accessible here. These overshoots were accompanied by an extra, slowly decaying mode in the temporal autocorrelation function of the scattered intensity and by a marked slowing of the response of the system's scattering behavior to temperature changes. Previous SANS experiments on binary-mixture–Vycor glass systems showed clear evidence of domains in the two-phase region of the pure system, in the form of bubbles of water-rich phase confined inside the pores, surrounded by a lutidine-rich phase in contact with the pore walls [9].

Evidence of phase separation was also observed in the present experiments at temperatures above the highest one for which data are shown in Fig. 3. The samples containing 37, 40, and 43 vol% lutidine were quenched

TABLE IV. Parameters resulting from fitting Eq. (16) to the data for the gel-mixture sample with $\bar{\phi}_l = 0.43$.

T (°C)	$\bar{\phi}_l^{\text{free}}$	χ (10^{-20} cm^3)	ξ (Å)	α_0	B (cm^{-1})
8.50	0.43	0.0149 ± 0.0033	13.5 ± 0.94	1.00 ± 0.004	0.578 ± 0.015
18.34	0.42	0.0880 ± 0.0080	23.2 ± 1.19	1.26 ± 0.005	0.607 ± 0.008
23.03	0.42	0.310 ± 0.027	38.3 ± 1.95	1.44 ± 0.006	0.560 ± 0.008
25.84	0.41	0.372 ± 0.026	37.1 ± 1.51	1.70 ± 0.007	0.475 ± 0.008
26.80	0.41	0.584 ± 0.029	43.6 ± 1.22	1.89 ± 0.006	0.461 ± 0.008
27.76	0.41	0.620 ± 0.054	46.1 ± 2.01	2.08 ± 0.011	0.394 ± 0.008
28.75		11.2 ± 0.50	191 ± 4.1	8.81 ± 0.17	0.427 ± 0.015
29.71		27.6 ± 2.30	342 ± 14.0	8.67 ± 0.45	0.575 ± 0.011

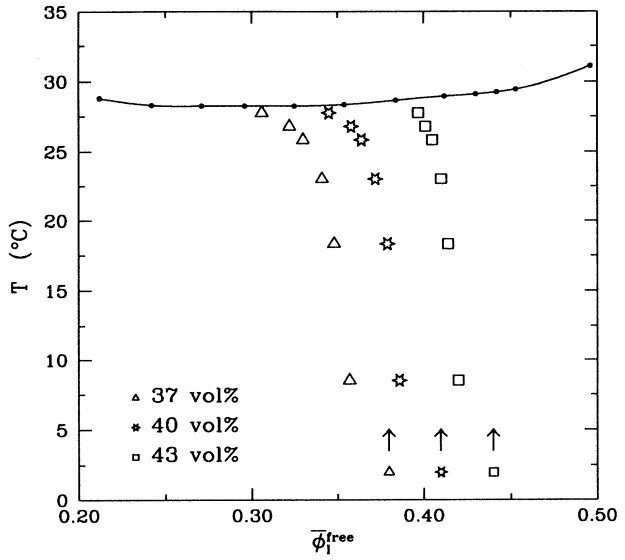

FIG. 5. Phase diagram of lutidine and D_2O showing estimated values of the lutidine concentration in the nonadsorbed or free fluid for various samples and temperatures. The average composition of the fluid portion of each sample is shown by the arrows. The solid points are the coexistence curve of the pure mixture as estimated by cloud point measurements; the solid line is a spline through this data. Results for samples containing 37 (△), 40 (∗), and 43 (□) vol% lutidine are shown. Preferential adsorption of lutidine results in strong variation of the free fluid concentration as the critical region is approached.

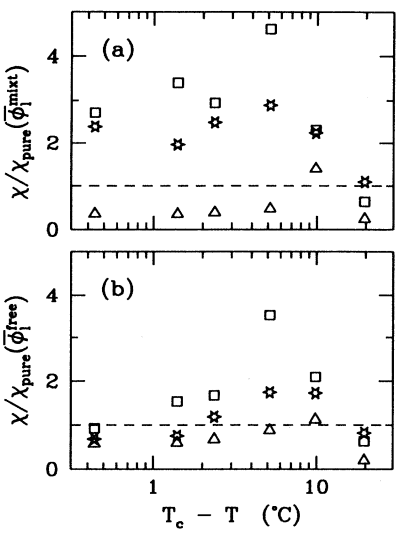

FIG. 7. Ratio of the susceptibility χ for gel-mixture samples containing 37 (△), 40 (∗), and 43 (□) vol% lutidine to that of the pure system at the same temperature. In (a) the comparison is made to the pure system at the mean composition of the fluid mixture in the gels $\bar{\phi}_l^{mixt}$. In (b) the comparison is made to the pure system at a temperature dependent concentration $\bar{\phi}_l^{free}$ estimated for the free, nonadsorbed fluid. The temperatures are relative to the critical temperature $T_c = 28.2\,^{\circ}C$ of the pure system.

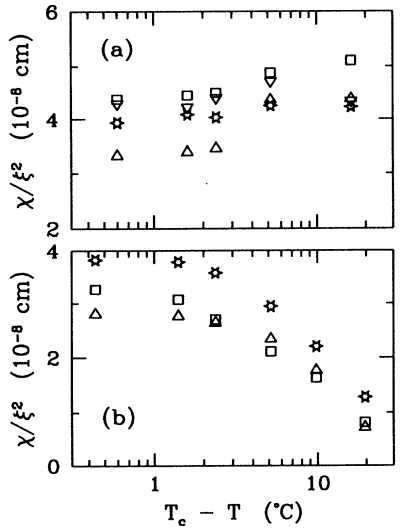

FIG. 6. Ratio of the susceptibility χ to the square of the correlation length ξ for (a) the pure system at four different samples containing 25.0 (△), 31.0 (∗), 35.0 (□), and 40.0 (▽) vol% lutidine and (b) for gel-mixture samples containing 37 (△), 40 (∗), and 43 (□) vol% lutidine. The temperatures are relative to the critical temperature $T_c = 28.2\,^{\circ}C$ of the pure system.

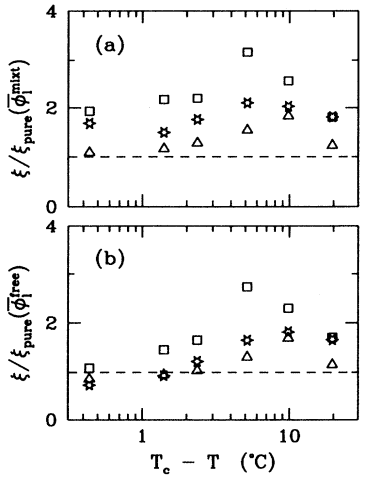

FIG. 8. Ratio of the correlation length ξ for gel-mixture samples containing 37 (△), 40 (∗), and 43 (□) vol% lutidine to that of the pure system at the same temperature. In (a) the comparison is made to the pure system at the mean composition of the fluid mixture in the gels $\bar{\phi}_l^{mixt}$. In (b) the comparison is made to the pure system at a temperature dependent concentration $\bar{\phi}_l^{free}$ estimated for the free, nonadsorbed fluid. The temperatures are relative to the critical temperature $T_c = 28.2\,^{\circ}C$ of the pure system.

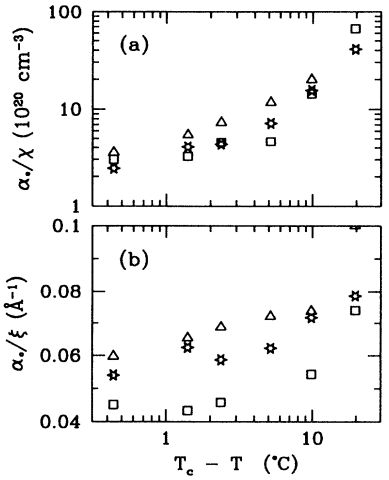

FIG. 9. Ratio of the long-wavelength limit of the response function $\alpha_0(T)$ to (a) the susceptibility χ and (b) the correlation length ξ of the three gel-mixture samples. Clearly $\alpha_0(T)$ does not diverge nearly as strongly as does χ; instead it seems to vary much more like ξ.

from 27.76 °C to 28.75 °C and subsequently to 29.71 and 34.57 °C, 4 and 11 h after the initial quench, respectively. Data taken at these temperatures for the sample containing 40 vol% lutidine are shown in Fig. 10. Data shown for temperatures of 28.75, 29.71, and 34.57 °C were taken 3, 5, and 7 h after changing the temperature to those respective values. Following temperature increases beyond 27.76 °C, the scattered intensity increased dramatically at low q, developing a q^{-4} dependence, as can be seen by comparing the data to the solid line, which has a slope of -4. In addition, this behavior was accompanied by a distinct change in structure at high q. Instead of remain-

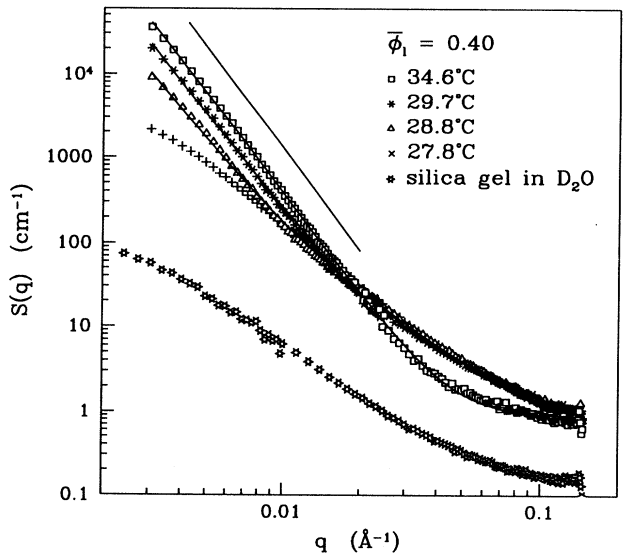

FIG. 10. Absolute neutron-scattering cross section per unit volume measured for the gel-mixture sample containing 2.05 vol% silica and 40 vol% lutidine at one temperature (27.76 °C) in the one-phase region and three temperatures (28.75, 29.71, and 34.57 °C) in the two-phase region. The line on the figure has a slope of -4, which is the result expected for scattering from a sample containing sharp interfaces. The solid lines through the data are fits of Eq. (20) to the data and the lower data set in each graph is the scattering from a gel containing only D_2O.

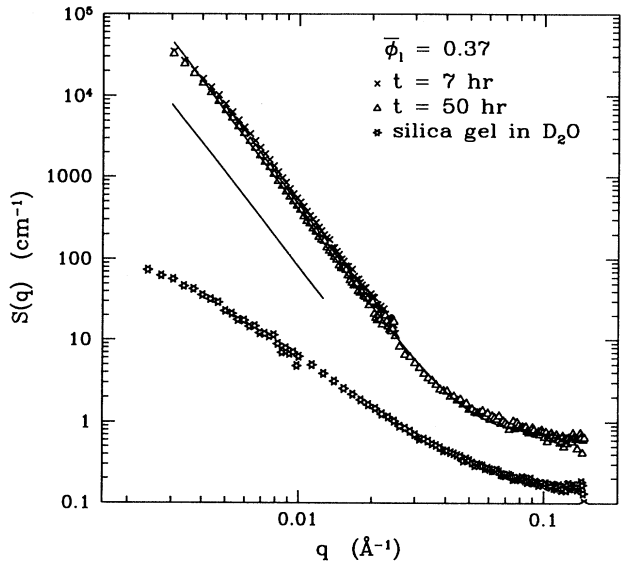

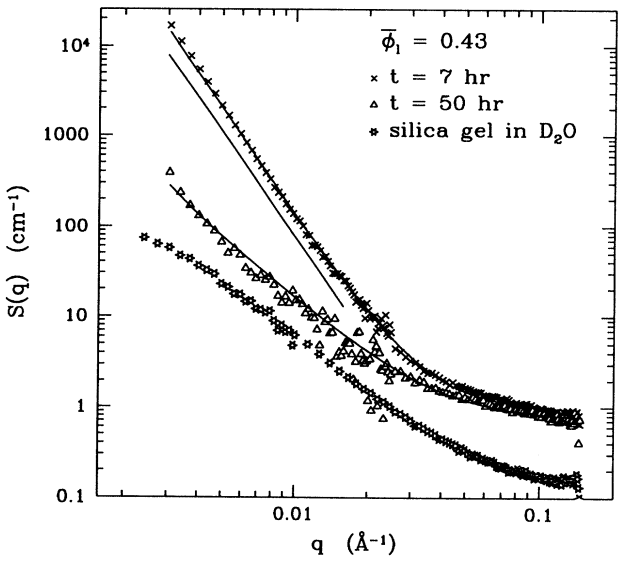

FIG. 11. Absolute neutron-scattering cross section per unit volume for samples containing (a) 37 and (b) 43 vol% lutidine at two different times after raising their temperatures to 34.57 °C, well into the two-phase region. The sample containing 37 vol% lutidine showed essentially no evolution during the duration of the experiment, while the one containing 43 vol% lutidine evolved significantly, presumably due to domain coarsening. The lower data set in each graph is the scattering from a gel containing only D_2O. The straight line on each figure has a slope of -4 and the solid lines through the data are fits of Eq. (20) to the data.

TABLE V. Parameters resulting from fitting Eq. (20) to the data for the gel-mixture sample with $\bar{\phi}_l = 0.37$.

T (°C)	δt (h)	B (cm^{-1})	C_1 (cm^{-1})	ξ_d (Å)	C_1^* (cm^{-5})	C_2
28.75	3	0.539±0.02	$(2.06\pm0.1)\times10^4$	319±4	5.63×10^{-8}	10.8±0.2
29.71	5	0.72±0.04	$(1.49\pm0.2)\times10^5$	482±16	2.76×10^{-6}	6.6±0.4
34.57	50	0.66±0.03			$(3.88\pm0.04)\times10^{-6}$	0.48±0.23

ing saturated at high q, the scattered intensity decreased below the saturated value, which had been observed in the one-phase region. If Eq. (16) is fit to the data, there is a discontinuous change in the fit parameters at temperatures beyond 27.76 °C, as can be seen in Tables II–IV.

The scattering cross section in the two-phase region was observed to evolve slowly with time, the initial increase in intensity being followed by a slow decrease, reminiscent of the overshoots observed in the light-scattering studies [10,11]. We studied the time dependence of the scattering behavior of a number of samples after their temperatures were raised beyond 27.76 °C. All samples showed a slow decrease in the low-q scattering following the initial increase, which occurred after the temperature was changed. In fact, during this time, the samples were gradually clearing visually and typically became clear after several days. However, this behavior was concentration dependent; samples of low lutidine concentration appeared to clear more slowly than those of high lutidine concentration. Figure 11 shows data taken for two samples raised and held at 34.57 °C, about 7 °C beyond where phase separation first appears to occur. Figure 11(a) shows the results observed for a sample containing 37 vol% lutidine. As may be seen, this sample showed very little evolution in its scattering cross section over the full 50-h duration of the experiment. Similar behavior was also observed in samples containing 22, 32, and 39 vol% lutidine, although slightly more evolution was observed in the 39 vol% sample. The behavior of a sample containing 43 vol% lutidine was considerably different however, as shown in Fig. 11(b). By late times the scattered intensity had decreased dramatically and the q^{-4} region at low q was no longer evident.

This behavior is consistent with the appearance and coarsening of lutidine-rich and water-rich domains in the gel sample. We model the scattering in what would be the two-phase region of the pure system as follows. Let us assume that domains of water-rich and lutidine-rich phase form with characteristic size ξ_d and scattering length densities ρ_1 and ρ_2, respectively, with smooth interfaces between them. As discussed by Debye *et al.* [32] in the case of a porous medium and in the context of domain scattering by Wong *et al.* [15] and Lin *et al.* [9], the scattering from such domains can be represented by a Lorentzian-squared term. If we further assume that the scattering from silica gel strands in a particular domain is determined by the *local* contrast and further that the domains scatter incoherently from each other, we are led to the following form for $S(q)$ in this region:

$$S(q) = B + \frac{C_1}{(1+q^2\,\xi_d^2)^2} + C_2\,S(q)_{ghw}, \tag{20}$$

where $C_1 \propto N\,(\rho_1-\rho_2)^2\,\xi_d^6$ for scattering from a binary system of N domains with contrast $(\rho_1-\rho_2)$ and average domain size ξ_d, as discussed in Ref. [9]. The first term B is a constant (incoherent scattering) background and C_2 is a constant given by

$$C_2 = \frac{[f_1(\rho_s'-\rho_1)^2 + f_2(\rho_s'-\rho_2)^2]}{(\rho_s-\rho_{hw})^2}, \tag{21}$$

where f_1, f_2 are the fractions of the silica gel in the water-rich and lutidine-rich domains, respectively. The third term in Eq. (20) has the same effect as the term involving α_0 in Eq. (14) in the limit of $\xi \to 0$. Preferential adsorption is incorporated into an effective ρ_s', which is smaller than the bare SiO_2 value as any adsorbed lutidine decreases the effective scattering length density of the silica gel. When this form was used to fit the data, ξ_d turned out to be sufficiently large in most cases that the second term becomes just the Porod (interface) scattering [28], in which case the second term in Eq. (20) was replaced by the term $C_1^*\,q^{-4}$, where C_1^* is proportional to $(\rho_1-\rho_2)^2\,A$ and A is the total interfacial area between domains.

The solid lines in Figs. 10 and 11 show the quality of fits of Eq. (20) to data for the samples containing 37, 40, and 43 vol% lutidine. Tables V–VII list the parameters C_1, ξ_d (where measurable), C_1^*, and C_2 for these temperatures. In these tables, δt refers to the time elapsed

TABLE VI. Parameters resulting from fitting Eq. (20) to the data for the gel-mixture sample with $\bar{\phi}_l = 0.40$.

T (°C)	δt (h)	B (cm^{-1})	C_1 (cm^{-1})	ξ_d (Å)	C_1^* (cm^{-5})	C_2
28.75	3	0.65±0.019			$(8.23\pm0.1)\times10^{-7}$	14.7±0.17
29.71	5	0.86±0.025			$(1.89\pm0.02)\times10^{-6}$	11.0± 0.21
34.57	7	0.86±0.02	$(2.2\pm1.2)\times10^7$	1550±220	3.79×10^{-6}	0.81±0.19
34.57	50	0.57±0.15			$(9.53\pm0.1)\times10^{-7}$	1.47±0.1

TABLE VII. Parameters resulting from fitting Eq. (20) to the data for the gel-mixture sample with $\bar{\phi}_l = 0.43$.

T (°C)	δt (h)	B (cm^{-1})	C_1 (cm^{-1})	ξ_d (Å)	C_1^* (cm^{-5})	C_2
28.75	3	0.64±0.01	(2.2±1.3) × 10^6	1200±187	1.04×10^{-6}	14.1±0.2
29.71	5	0.74±0.02			(2.49±0.08) × 10^{-7}	10.3±0.2
34.57	7	0.89±0.15			(1.23±0.02) × 10^{-6}	1.98± 0.11
34.57	50	0.72±0.01			(1.35±0.1) × 10^{-8}	2.27± 0.058

since the temperature was changed. For cases where ξ_d was obtained directly from the fits, C_1^* was calculated as $C_1^* = C_1/\xi_d^4$. From the fit results, one may see that C_1^* generally increases as one quenches deeper into this region. Furthermore, with the passage of time, the parameter C_1^* decreases, presumably due to coarsening of the domains, and thus a decreased interfacial area. The magnitude of C_2 illustrates the importance of adsorption even in what would be the two-phase region of the pure system; the contrast of the lutidine-rich and water-rich domains to bare SiO_2 would require C_2 to be at least an order of magnitude smaller. The constant C_2 decreases as the samples are quenched deeper into the two-phase region. This is probably because the amount of adsorbed lutidine is decreasing as the sample moves farther away from the critical point, decreasing the contrast between the silica gel with its adsorbed lutidine layer and the lutidine-rich and water-rich domains. It is also significant that the length scale associated with these domains is typically large compared to the largest meaningful length-scale measurable with the SANS configuration, which is about 1500 Å. This length scale is considerably larger than ξ_G, the length scale over which fluctuations in silica concentration are correlated in the gel. Presumably this means that the domains are large enough to encompass many gel strands. In contrast, experiments on binary mixtures in Vycor glass show that the phase-separating domains never grow larger than the characteristic pore size of this material [9].

IV. CONCLUSIONS

The neutron-scattering studies of silica gels made in D_2O reported here show that the fractal nature of these gels continues to the smallest length scales probed (~10 Å). The variation of the gel correlation length with concentration and pH is consistent with previous light-scattering studies. The fractal dimension as determined by fits to the scattering cross sections of all of the gels reported here is consistent with $D_f = 2.1 \pm 0.1$.

Studies of the gel-mixture samples in the one-phase region show several interesting features. Even well away from the phase boundary of the pure system, the scattering from the gel-mixture samples shows a strong response of the mixture to the fluctuations in silica concentration, over the entire range of length scales studied here. As the temperature approaches the phase boundary of the pure system, the response saturates on small length scales. A scattering function incorporating both critical fluctuations and a q-dependent static response was fit to the data. These fits show that the length scale associated with the static response is not distinguishable from that associated with the critical fluctuations to within the present accuracy. However, the amplitude of the response is clearly not proportional to the susceptibility of the mixture, as it would be for linear response. The interpretation of the data in the present study is similar to that used to analyze neutron-scattering data for field-cooled random-field magnets in the paramagnetic phase with two main differences: the correlated nature of the gel structure results in a slightly more complicated fitting function and neutron-scattering studies of field-cooled random-field magnets [33] are consistent with a response to the field proportional to the staggered susceptibility (linear response). Further analysis of the present system shows that the correlation length and susceptibility of the free fluid are found to be comparable to those of the pure or unconfined system, provided the comparison is made to the pure system at the concentration estimated for the free fluid rather than at the average concentration.

Studies of the gel-mixture samples in the two-phase region reveal quantitative evidence for the existence of domains corresponding to lutidine-rich and water-rich phases. This is reminiscent of the domains observed in field-cooled antiferromagnets doped with nonmagnetic impurities. For the gel-mixture system the domains coarsen noticeably with time and their size is considerably larger than the distance over which fluctuations in silica concentration are correlated. The time scale of the coarsening process changes dramatically with concentration, which is intriguing but unexplained.

ACKNOWLEDGMENTS

This research was supported by NSF Grants Nos. DMR91-22444, DMR90-18089, and DMR93-20726 and NSERC Canada. The authors acknowledge helpful discussions with P.-Z. Wong. We also acknowledge the support of the National Institute of Standards and Technology, U.S. Department of Commerce, and EXXON Research and Engineering in providing the facilities used in this experiment. B.J.F. gratefully acknowledges the assistance of K. Christie in measurement of the lutidine-D_2O coexistence curve.

[1] M.E. Fisher, in *Critical Phenomena*, edited by F.J.W. Hahne (Springer-Verlag, New York, 1983).
[2] D.S. Fisher, G.M. Grinstein, and A. Khurana, Phys. Today **41** (12), 56 (1988), and references therein.
[3] B.J. Frisken, A.J. Liu, and D.S. Cannell, Mater. Res. Bull. **19**, 19 (1994), and references therein.
[4] F. Brochard and P.G. de Gennes, J. Phys. Lett. **44**, L785 (1983).
[5] A.P.Y. Wong and M.H.W. Chan, Phys. Rev. Lett. **65**, 2567 (1990); A.P.Y. Wong, S.B. Kim, J. Ma, W.I. Goldburg, and M.H.W. Chan, *ibid.* **70**, 954 (1993).
[6] Z. Zhuang, A.G. Casielles, and D.S. Cannell (unpublished).
[7] J.V. Maher, W.I. Goldburg, D.W. Pohl, and M. Lanz, Phys. Rev. Lett. **53**, 60 (1984); K.-Q. Xia and J.V. Maher, Phys. Rev. A **36**, 2432 (1987); **37**, 3626 (1988); W.I. Goldburg, in *Scaling Phenomena in Disordered Systems*, edited by R. Pynn and A. Skjeltorp (Plenum, New York, 1985), p. 151; M.C. Goh, W.I. Goldburg, and C.M. Knobler, Phys. Rev. Lett. **58**, 1008 (1987); F. Aliev, W.I. Goldburg, and X-l. Wu, Phys. Rev. E **47**, R3834 (1993).
[8] S.B. Dierker and P. Wiltzius, Phys. Rev. Lett. **58**, 1865 (1987), P. Wiltzius, S.B. Dierker, and B.S. Dennis, *ibid.* **62**, 804 (1989); S.B. Dierker and P. Wiltzius, *ibid.* **66**, 1185 (1991).
[9] M.Y. Lin, S.K. Sinha, J.M. Drake, X.-l. Wu, P. Thiyagarajan, and H.B. Stanley, Phys. Rev. Lett. **72**, 2207 (1994).
[10] B.J. Frisken, F. Ferri, and D.S. Cannell, Phys. Rev. Lett. **66**, 2754 (1991).
[11] B.J. Frisken and D.S. Cannell, Phys. Rev. Lett. **69**, 632 (1992).
[12] N. Mulders, R. Mehrotra, L.S. Goldner, and G. Ahlers, Phys. Rev. Lett. **67**, 695 (1991), and references therein.
[13] P.G. de Gennes, J. Phys. Chem. **88**, 6469 (1984).
[14] D. Andelman and J.-F. Joanny, in *Scaling Phenomena in Disordered Systems*, Vol. 133 of *NATO Advanced Study Institute, Series B: Physics*, edited by R. Pynn and A. Skjeltorp (Plenum, New York, 1985), p. 163.
[15] P. Wong, J.W. Cable, and P. Dimon, J. Appl. Phys. **55**, 2377 (1984).
[16] R.J. Birgeneau, R.A. Cowley, G. Shirane, and H. Yoshizawa, J. Stat. Phys. **34**, 817 (1984).
[17] V. Jaccarino and A.R. King, Physica A **163**, 291 (1990), and references therein.
[18] D.P. Belanger and A.P. Young, J. Magn. Magn. Mater. **100**, 272 (1991).
[19] L. Monette, A.J. Liu, and G.S. Grest, Phys. Rev. A **46**, 7664 (1992).
[20] A.J. Liu, D.J. Durian, E. Herbolzheimer, and S.A. Safran, Phys. Rev. Lett. **65**, 1897 (1990).
[21] A. Maritan, M.R. Swift, M. Cieplak, M.H.W. Chan, M.W. Cole, and J.R. Banavar, Phys. Rev. Lett. **67**, 1821 (1991).
[22] F. Ferri, B.J. Frisken, and D.S. Cannell, Phys. Rev. Lett. **67**, 3626 (1991).
[23] For a general review of critical behavior at surfaces, please see K. Binder, in *Phase Transitions and Critical Phenomena*, edited by C. Domb and J.L. Lebowitz (Academic, London, 1986), Vol. X, p. 75.
[24] M.E. Fisher and P.-G. de Gennes, C.R. Acad. Sci. Paris **287**, 207 (1978).
[25] D. Avnir and V.R. Kaufman, J. Non-Cryst. Solids **92**, 180 (1987); B. Cabane, M. Dubois, F. Lefaucheux, and M.C. Robert, *ibid.* **119**, 121 (1990).
[26] S.K. Sinha, T. Freltoft, and J. Kjems, in *Kinetics of Aggregation and Gelation*, edited by F. Family and D.P. Landau (North-Holland, Amsterdam, 1984), p. 87; T. Freltoft, J.K. Kjems, and S.K. Sinha, Phys. Rev. B **33**, 269 (1986).
[27] The measured scattering cross section is the convolution of the true differential scattering cross section with the instrumental response function. The instrumental response is broadened both by the wavelength spread of the incident neutrons and by the range of directions they take in passing through the sample. The resulting fractional spread in the scattering wave vector ranged from 0.24 at low q to 0.14 at high q. We estimated the effect such spread would have on the fit parameters deduced from the data by fitting the data to the theoretical form convolved with a rectangular response function of fractional width 0.24. Since none of the deduced parameters varied by more than 3% when the instrumental response was included, we did not include it in our fits to any of the data, either for gels or gel-mixture systems.
[28] G. Porod, in *Small Angle Xray Scattering*, edited by O. Glatter and O. Kratky (Academic, New York, 1982), p. 44.
[29] R.F. Chang, H. Burstyn, and J.V. Sengers, Phys. Rev. A **19**, 866 (1979).
[30] B.J. Frisken, F. Ferri, and D.S. Cannell, in *Dynamics in Small Confining Systems*, edited by J.M. Drake, J. Klafter, R. Kopelman, and D.D. Awschalom, MRS Symposia Proceedings No. 290 (Materials Research Society, Pittsburgh, 1993), p. 59.
[31] In the previous light-scattering work, the adsorbed fluid was *defined* to be that responsible for the enhanced static scattering.
[32] P. Debye, H.R. Anderson, and H. Brumberger, J. Appl. Phys. **28**, 679 (1957).
[33] D.P. Belanger, A.R. King, and V. Jaccarino, Phys. Rev. B **31**, 4538 (1985).